[redacted] 70279 Copy 403



NASA MEMO 4-10-59L

# NASA

# MEMORANDUM

Declassified by authority of NASA
Classification Change Notices No. 214
Dated 30 SEP 1971

EFFECTS OF FOREBODY LENGTH AND CANARD-SURFACE SIZE ON THE STABILITY AND CONTROL CHARACTERISTICS OF A 70° DELTA-WING CANARD AIRPLANE CONFIGURATION AT A MACH NUMBER OF 2.01

By M. Leroy Spearman and Cornelius Driver

Langley Research Center
Langley Field, Va.

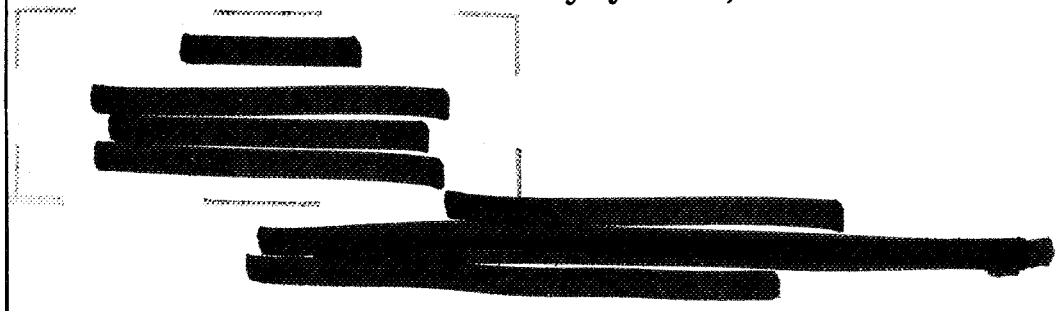

## NATIONAL AERONAUTICS AND SPACE ADMINISTRATION

WASHINGTON
March 1959

[redacted]

DECLASSIFIED

NATIONAL AERONAUTICS AND SPACE ADMINISTRATION

MEMORANDUM 4-10-59L

# EFFECTS OF FOREBODY LENGTH AND CANARD-SURFACE SIZE ON THE STABILITY AND CONTROL CHARACTERISTICS OF A 70° DELTA-WING CANARD AIRPLANE CONFIGURATION AT A MACH NUMBER OF 2.01*

By M. Leroy Spearman and Cornelius Driver

L 1 9 6

## SUMMARY

An investigation has been conducted in the Langley 4- by 4-foot supersonic pressure tunnel at a Mach number of 2.01 to determine the stability and control characteristics of canard airplane configurations equipped with a 70° delta wing. The configurations investigated included two bodies with length-diameter ratios of 11.1 and 12.5 and two 70° delta canard surfaces with ratios of exposed area to wing total area of 0.075 and 0.126. The models were equipped with twin swept wing-mounted vertical tails. The tests were made through a range of combined angle of attack and sideslip from 0° to about 20° with control deflections ranging from 0° to 15°.

When the body length or canard-surface size was increased, the maximum trim lift-drag ratio decreased at low stability levels and increased at high stability levels. The experimentally determined variations of control effectiveness $C_{m_\delta}$ and longitudinal stability $\partial C_m/\partial C_L$ with canard volume coefficient were in reasonably close agreement with estimated variations.

The directional-stability parameter $C_{n_\beta}$ was smaller with the longer body, primarily because of the increase in instability of the body. With increasing angle of attack, an increase in $C_{n_\beta}$ occurred with increasing canard size because of a decrease in the instability of the tail-off configuration and an increase in the tail contribution. The decrease in tail-off instability was probably caused by a strake effect of the canard surface on the forebody pressures, whereas the increase in tail contribution was probably caused by an increase in strength of the favorable sidewash in the region of the twin vertical tails.

*Title, Unclassified.

## INTRODUCTION

A research program is underway at the Langley 4- by 4-foot supersonic pressure tunnel to determine the aerodynamic characteristics of several canard airplane configurations. Various phases of the program are presented in references 1 to 6. As a part of this program, an investigation has been made at a Mach number of 2.01 to determine some effects of forebody length and canard-surface size on the aerodynamic characteristics of a configuration having a 70° delta wing and canard surface and twin wing-mounted swept vertical tails.

Increasing the forebody length could serve a twofold purpose in providing increased body volume and a longer moment arm for the canard surface. In addition, increasing the size of the canard surface should provide an increase in controllability. However, a limiting factor to consider might be the tendency toward increased longitudinal and directional instability as the forebody length is increased. In addition, some changes in the interference effects of the forebody and canard flow fields on the wing and vertical tail might be expected as the forebody length and canard-surface size are varied. The purpose of the present investigation was to determine the extent to which the longitudinal and lateral stability and control characteristics of a generalized canard configuration might be affected by changes in the forebody length and canard-surface size. Two different forebody lengths and two canard-surface sizes were investigated.

## SYMBOLS

The results are presented as force and moment coefficients with lift, drag, and pitching-moment coefficients referred to the stability-axis system and rolling-moment, yawing-moment, and side-force coefficients referred to the body-axis system. The reference center of moments was on the body center line at a point 12 inches forward of the base for all models (21.7 percent of wing mean geometric chord).

| | |
|---|---|
| $b$ | wing span |
| $\bar{c}$ | wing mean geometric chord |
| $C_D$ | drag coefficient, $\frac{\text{Drag}}{qS}$ |
| $C_L$ | lift coefficient, $\frac{\text{Lift}}{qS}$ |

UNCLASSIFIED



| | |
|---|---|
| $C_l$ | rolling-moment coefficient, $\frac{\text{Rolling moment}}{qSb}$ |
| $C_{l_\beta}$ | effective-dihedral parameter, $\partial C_l/\partial\beta$ |
| $C_m$ | pitching-moment coefficient, $\frac{\text{Pitching moment}}{qS\bar{c}}$ |
| $\partial C_m/\partial C_L$ | longitudinal-stability parameter (measured at low lift coefficients and $\delta_c = 0^o$) |
| $C_{m_\delta}$ | canard pitching effectiveness at $\alpha = 0^o$, $\partial C_m/\partial\delta_c$ |
| $C_n$ | yawing-moment coefficient, $\frac{\text{Yawing moment}}{qSb}$ |
| $C_{n_\beta}$ | directional-stability parameter, $\partial C_n/\partial\beta$ |
| $C_Y$ | side-force coefficient, $\frac{\text{Side force}}{qS}$ |
| $C_{Y_\beta}$ | side-force parameter, $\partial C_Y/\partial\beta$ |
| L/D | lift-drag ratio |
| $l$ | distance from canard-surface hinge line to reference center of moments |
| q | free-stream dynamic pressure |
| S | wing area including body intercept |
| $S_c$ | exposed area of canard surface |
| $\frac{S_c l}{S\bar{c}}$ | canard volume coefficient |
| $\alpha$ | angle of attack, deg |
| $\beta$ | angle of sideslip, deg |
| $\delta_c$ | angle of canard deflection, deg |

[redacted]

Subscripts:

| | |
|---|---|
| max | maximum value |
| trim | value at $C_m = 0$ |

Component designations:

| | |
|---|---|
| B | body |
| C | canard surface |
| L | large |
| S | small |
| V | vertical tail |
| W | wing |

## MODELS AND APPARATUS

Details of the models are shown in figure 1 and the geometric characteristics are presented in table I. A photograph of one of the models is presented in figure 2. Coordinates of the bodies are given in table II. The two body lengths were obtained by inserting cylindrical center-body adapters of different lengths between a common forebody and afterbody. The canard-surface hinge line was fixed with respect to the forebody and hence the canard surface moved forward with the forebody as the overall body length was increased. The canard surface was motor driven and the deflections were set by remote control.

Force and moment measurements were made through the use of a six-component internal strain-gage balance. The model was mounted in the tunnel on a remote-controlled rotary sting.

## TESTS AND CORRECTIONS

The tests were made in the Langley 4- by 4-foot supersonic pressure tunnel at a Mach number of 2.01, a stagnation pressure of 10 pounds per square inch absolute, and a stagnation temperature of 100° F. The stagnation dewpoint was maintained sufficiently low (-25° F or less) to avoid significant condensation effects in the test section.

The angles of attack and sideslip were corrected for deflection of the balance and sting under load. The body base pressure was measured and the drag force was adjusted to a base pressure equal to free-stream static pressure.

The estimated variations in the individual measured quantities, based only on zero shifts and repeatability, are as follows:

| | |
|---|---|
| $C_L$ | ±0.0003 |
| $C_D$ | ±0.0010 |
| $C_m$ | ±0.0004 |
| $C_l$ | ±0.0004 |
| $C_n$ | ±0.0001 |
| $C_Y$ | ±0.0015 |

The maximum probable error in the angles of attack and sideslip is ±0.2°. The canard deflection angle was set to within ±0.1°. The Mach number is accurate to within ±0.01.

## DISCUSSION

### Longitudinal Stability

The aerodynamic characteristics in pitch for various combinations of component parts are shown in figure 3. These results are presented for a constant moment-center location with respect to the body base. Thus the level of longitudinal stability decreases both with an increase in forebody length and with an increase in canard-surface size. Each of the configurations indicates a tendency toward decreased stability with increasing lift, the tendency being slightly greater for the long body. The addition of the twin vertical tails results in a positive increment of pitching moment throughout the angle-of-attack range. This positive pitching moment is due in part to the increment in drag caused by the tails and in part to a decrease in wing lift caused by interference pressures transmitted from the vertical tails to the upper surface of the wing.

Since the addition of the vertical tails not only increases the drag but also decreases the lift, there is a marked reduction in L/D due to the tails. A further loss in L/D occurs with the addition of the canard surfaces, primarily because of an increase in drag (figs. 3 and 4). The effects of canard-control deflection on the aerodynamic characteristics in pitch for the various configurations (fig. 4) indicate

that progressive deflection of the canard control results in a progressive decrease in L/D because of further increases in drag.

Since these results are shown for a constant moment-center location with respect to the body base, an increase in forebody length or in canard-surface size results in an increase in canard pitching effectiveness $C_{m_\delta}$ and a decrease in static longitudinal stability $\partial C_m/\partial C_L$. The variations of $C_{m_\delta}$ and $\partial C_m/\partial C_L$ with canard volume coefficient are shown in figure 5. The estimated variations were obtained by the use of reference 7 but do not include effects of the canard-surface flow field on the wing.

For these configurations the variation of $C_{m_\delta}$ with canard volume coefficient is essentially linear and independent of whether the volume coefficient is changed by varying the forebody length or the canard size. The experimental and estimated values of $C_{m_\delta}$ are in good agreement.

Although there are differences in the experimental and estimated values of $\partial C_m/\partial C_L$, the variation of $\partial C_m/\partial C_L$ with canard volume coefficient is predicted reasonably well. The variation of $\partial C_m/\partial C_L$ with volume coefficient is essentially the same for both body lengths but, for a given volume coefficient, the level of stability is generally lower for the long body than for the short body.

The maximum trim value of L/D as a function of stability level is shown in figure 6 for each configuration. As would be expected, the maximum trim L/D decreases with an increase in stability level for each configuration. While the differences in L/D between the various configurations are small, at low stability levels the values of maximum trim L/D are generally higher for configurations with the short body or the small canard surface, whereas at high stability levels the values of maximum trim L/D are generally higher for configurations having the long body or the large canard surface. This trend might be expected since for low stability levels, where little control deflection is required for trimming, L/D is favorably influenced by the lower minimum drag of the configurations with the short body or the small canard surface. For high stability levels, where considerable control deflection is required for trimming, L/D is favorably influenced by the smaller control deflection angles required for configurations with the long body (long control moment arm) or the large canard surface.

## Lateral and Directional Stability

The effects of canard-surface size on the sideslip derivatives throughout the angle-of-attack range are shown in figure 7 for both body

lengths. The sideslip derivatives were obtained for the angle-of-sideslip range between 0° and 4° from measurements made through the angle-of-sideslip range at approximately 4° increments of angle of attack. The primary effect of increasing the canard-control size is to increase the directional stability $C_{n_\beta}$ at high angles of attack. The increase in $C_{n_\beta}$ is due in part to a decrease in the instability of the tail-off configuration and in part to an increase in the tail contribution to directional stability. The reduction in the tail-off instability at high angles of attack is probably due to a strake effect accompanying the increased root chord length of the large canard surface. As pointed out in reference 8, the use of forebody strakes provides directionally stabilizing pressures over the forebody. The increase in the tail contribution to directional stability with increasing canard-control size is probably caused by an increase in sidewash strength, since the vertical tails are located in a favorable sidewash region. Increasing the canard-surface size also causes a small increase in the positive dihedral effect $-C_{l_\beta}$ for the configuration, both with and without the vertical tails. In general, the effects of canard-surface size on the sideslip derivatives are the same for both body lengths.

The effects of body length on the sideslip derivatives throughout the angle-of-attack range are shown in figure 8 for both canard-surface sizes. The primary effect of increasing the body length is to decrease the directional stability throughout the angle-of-attack range for configurations either with or without the vertical tails. This is due in part to the fact that the moment-center location is constant with respect to the body base, and thus the body becomes more unstable as the forebody length is increased. In addition, the vertical-tail contribution, particularly at high angles of attack, becomes slightly smaller for the long body. This may result from a small decrease in the favorable sidewash effects as the canard surface is moved farther forward.

Lengthening the body had little effect on $C_{l_\beta}$ other than to cause a slight decrease in the positive dihedral effect at high angles of attack.

## CONCLUSIONS

An investigation has been made in the Langley 4- by 4-foot supersonic pressure tunnel at a Mach number of 2.01 to determine the effects of body length and canard-surface size on the stability and control characteristics of airplane configurations equipped with a wing and canard surfaces of 70° delta plan form. The configurations investigated included bodies having length-diameter ratios of 11.1 and 12.5 and canard surfaces

having ratios of exposed area to wing total area of 0.075 and 0.126. The results of the investigation indicated the following:

1. At low stability levels the maximum trim values of lift-drag ratio were generally higher for configurations with the short body or the small canard surface, whereas at high stability levels the maximum trim values of lift-drag ratio were generally higher for configurations with the long body or the large canard surface.

2. The variations of control effectiveness $C_{m_\delta}$ and longitudinal stability $\partial C_m/\partial C_L$ with canard volume could be predicted reasonably well by the use of existing estimating procedures.

3. The directional stability $C_{n_\beta}$ decreased with increasing body length primarily because of the increase in instability of the body.

4. The directional-stability parameter $C_{n_\beta}$ increased at high angles of attack as the canard-surface size was increased because of an increase in tail contribution and a decrease in tail-off instability. The decrease in tail-off instability probably resulted from a strake effect of the canard surface on the forebody pressures, whereas the increase in tail contribution was probably a result of an increase in the favorable sidewash in the region of the twin vertical tails.

Langley Research Center,
National Aeronautics and Space Administration,
Langley Field, Va., January 13, 1959.

UNCLASSIFIED



REFERENCES

1. Driver, Cornelius: Longitudinal and Lateral Stability and Control Characteristics of Two Canard Airplane Configurations at Mach Numbers of 1.41 and 2.01. NACA RM L56L19, 1957.

2. Spearman, M. Leroy, and Driver, Cornelius: Effects of Canard Surface Size on Stability and Control Characteristics of Two Canard Airplane Configurations at Mach Numbers of 1.41 and 2.01. NACA RM L57L17a, 1958.

3. Spearman, M. Leroy, and Driver, Cornelius: Longitudinal and Lateral Stability and Control Characteristics at Mach Number 2.01 of a 60° Delta-Wing Airplane Configuration Equipped With a Canard Control and With Wing Trailing-Edge Flap Controls. NACA RM L58A20, 1958.

4. Driver, Cornelius: Longitudinal and Lateral Stability and Control Characteristics of Various Combinations of the Component Parts of Two Canard Airplane Configurations at Mach Numbers of 1.41 and 2.01. NASA MEMO 10-1-58L, 1958.

5. Spearman, M. Leroy, and Driver, Cornelius: Some Factors Affecting the Stability and Performance Characteristics of Canard Aircraft Configurations. NACA RM L58D16, 1958.

6. Spearman, M. Leroy, and Driver, Cornelius: Effects of Forebody Length on the Stability and Control Characteristics at a Mach Number of 2.01 of a Canard Airplane Configuration With a Trapezoidal Aspect-Ratio-3 Wing. NASA MEMO 10-14-58L, 1958.

7. Pitts, William C., Nielsen, Jack N., and Kaattari, George E.: Lift and Center of Pressure of Wing-Body-Tail Combinations at Subsonic, Transonic, and Supersonic Speeds. NACA Rep. 1307, 1957.

8. Driver, Cornelius: Wind-Tunnel Investigation at a Mach Number of 2.01 of Forebody Strakes For Improving Directional Stability of Supersonic Aircraft. NACA RM L58C11, 1958.

L 1 9 6

TABLE I.- GEOMETRIC CHARACTERISTICS OF MODELS

| | Long | Short |
|---|---|---|
| **Body:** | | |
| Maximum diameter, in. | 3.33 | 3.33 |
| Length, in. | 41.5 | 37.0 |
| Base area, sq in. | 8.71 | 8.71 |
| Fineness ratio | 12.5 | 11.1 |
| **Wing:** | | |
| Span, in. | 16.72 | |
| Root chord at body center line, in. | 22.97 | |
| Tip chord, in. | 0 | |
| Area, sq in. | 192 | |
| Aspect ratio | 1.46 | |
| Taper ratio | 0 | |
| Mean geometric chord, in. | 15.33 | |
| Sweep angle of leading edge, deg | 70 | |
| Thickness, percent chord | 2.5 | |
| Section | Hexagonal | |
| **Canard surface:** | Large | Small |
| Total exposed area, sq in. | 24.1 | 14.44 |
| Ratio of exposed area to wing area | 0.126 | 0.075 |
| Section | Hexagonal | Hexagonal |
| Constant thickness, in. | 0.3125 | 0.3125 |
| Sweep angle of leading edge, deg | 70 | 70 |
| **Vertical tail:** | | |
| Total exposed area (both panels), sq in. | 46.84 | |
| Sweep angle of leading edge, deg | 60 | |
| Panel aspect ratio | 1.11 | |
| Taper ratio | 0.314 | |
| Section | Wedge-slab | |
| Leading-edge angle measured in plane normal to leading edge, deg | 10.6 | |
| Constant thickness, in. | 0.1875 | |

TABLE II.- BODY COORDINATES

| Station, in. | Radius, in. |
|---|---|
| Forebody | |
| 0 | 0 |
| .297 | .076 |
| .627 | .156 |
| .956 | .233 |
| 1.285 | .307 |
| 1.615 | .378 |
| 1.945 | .445 |
| 2.275 | .509 |
| 2.605 | .573 |
| 2.936 | .627 |
| 3.267 | .682 |
| 3.598 | .732 |
| 3.929 | .780 |
| 4.260 | .824 |
| 4.592 | .865 |
| 4.923 | .903 |
| 5.255 | .940 |
| 5.587 | .968 |
| 5.920 | .996 |
| 6.252 | 1.020 |
| 6.583 | 1.042 |
| Short body | |
| 17.75 | 1.667 |
| 37.00 | 1.667 |
| Long body | |
| 17.75 | 1.667 |
| 41.50 | 1.667 |

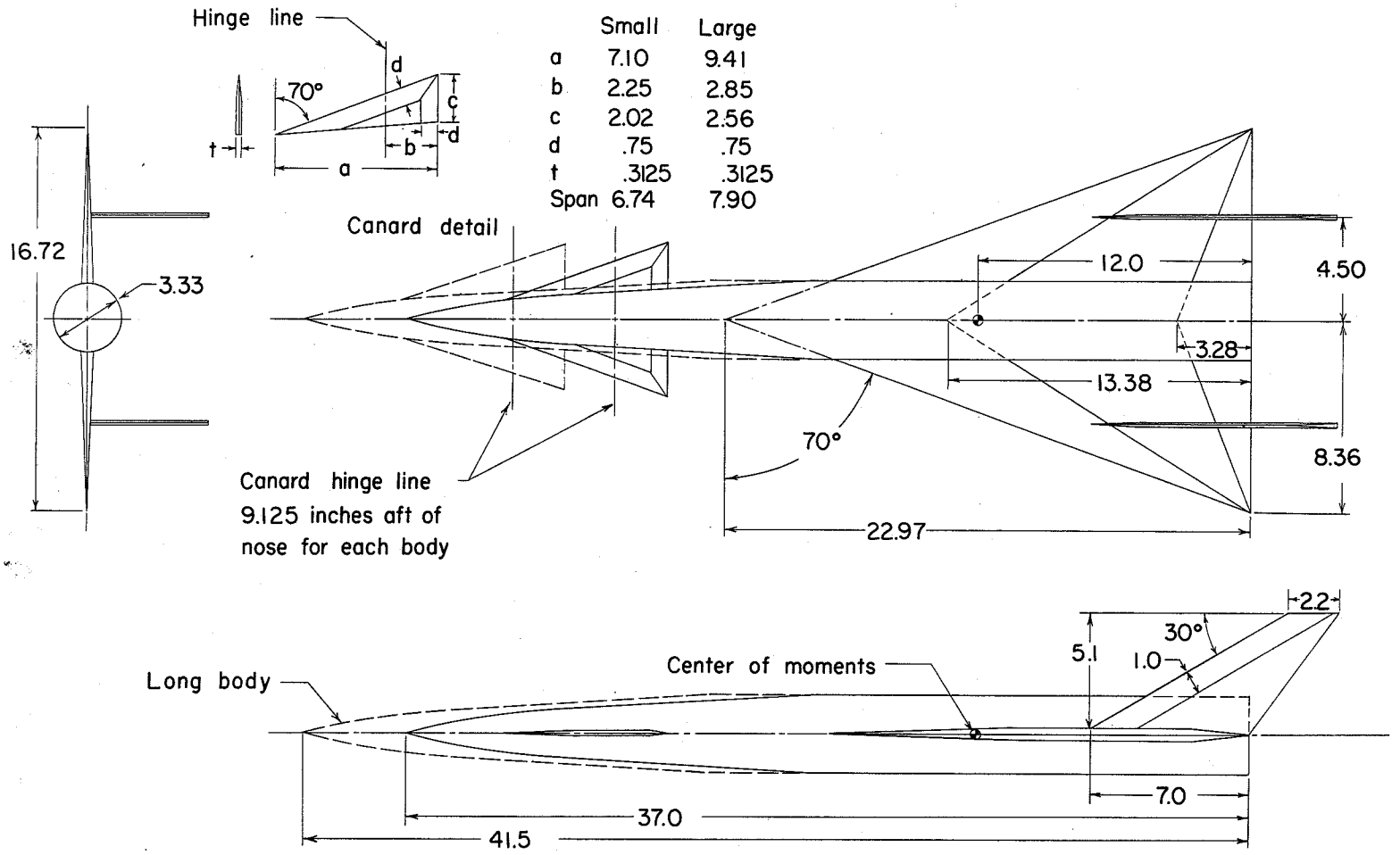


Figure 1.- Details of model. Linear dimensions are in inches.

Figure 2.- Model with long body and large canard surface. L-57-5276

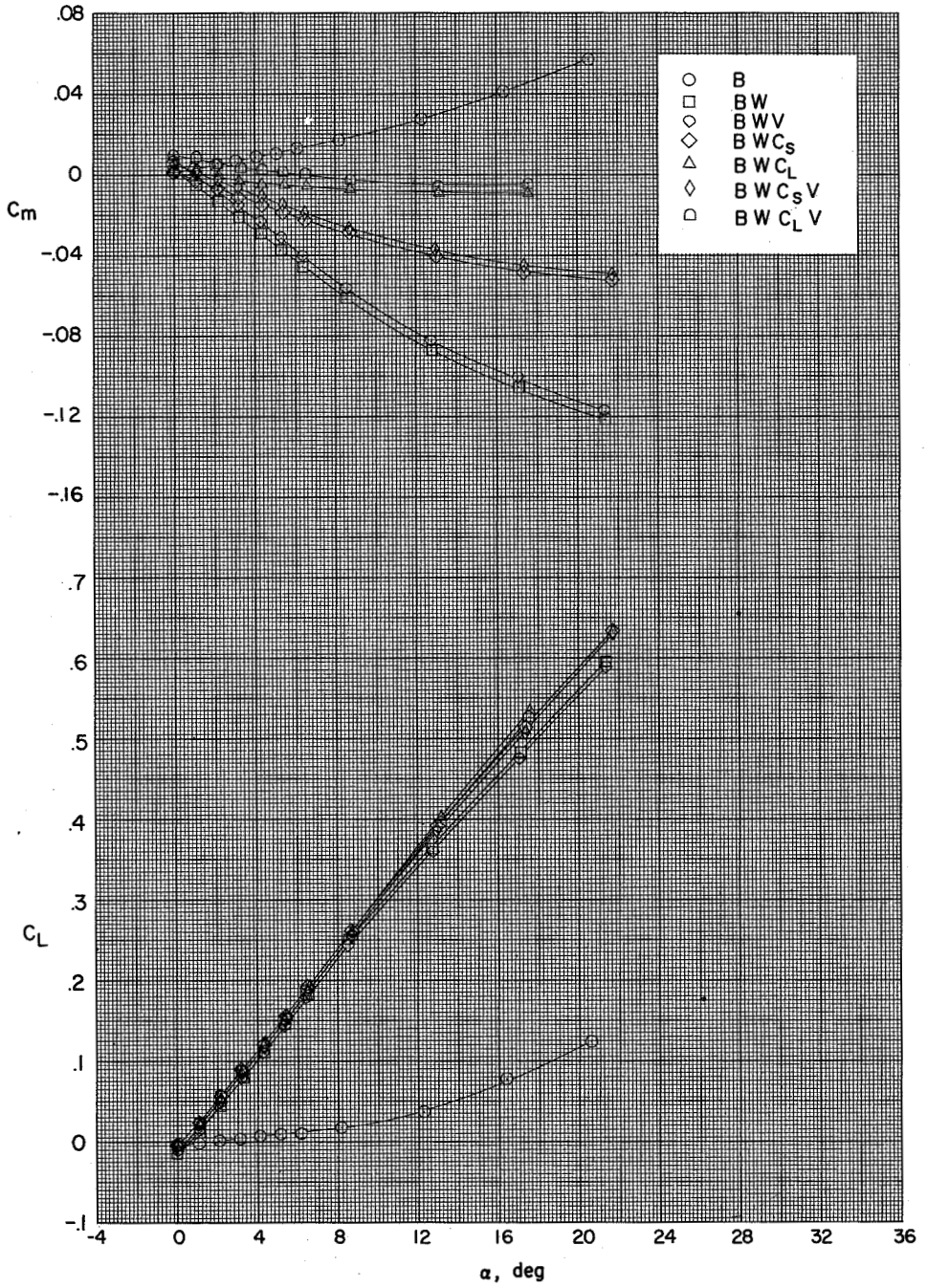


(a) Short body.

Figure 3.- Aerodynamic characteristics in pitch for various combinations of component parts.

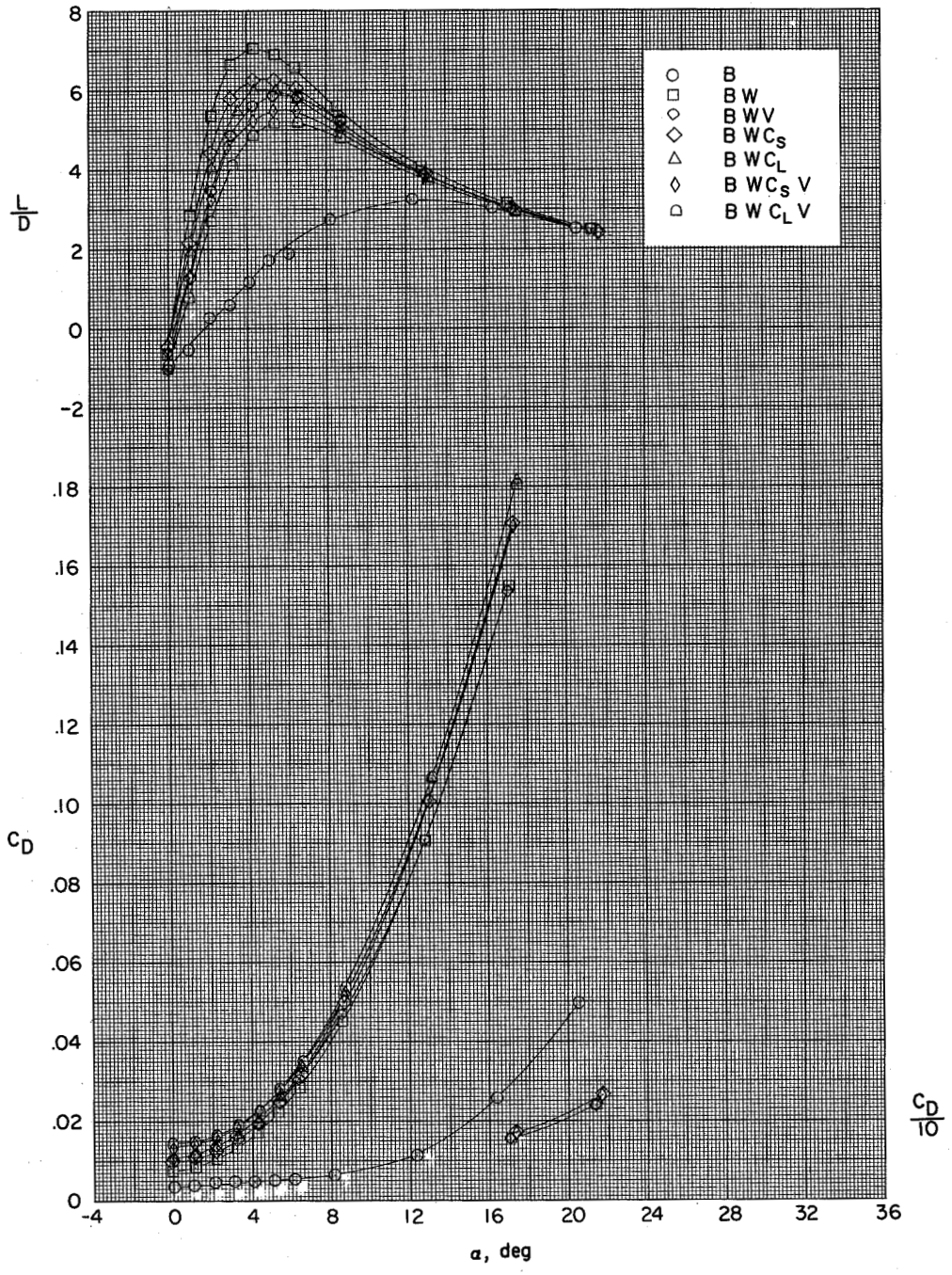


(a) Concluded.

Figure 3.- Continued.

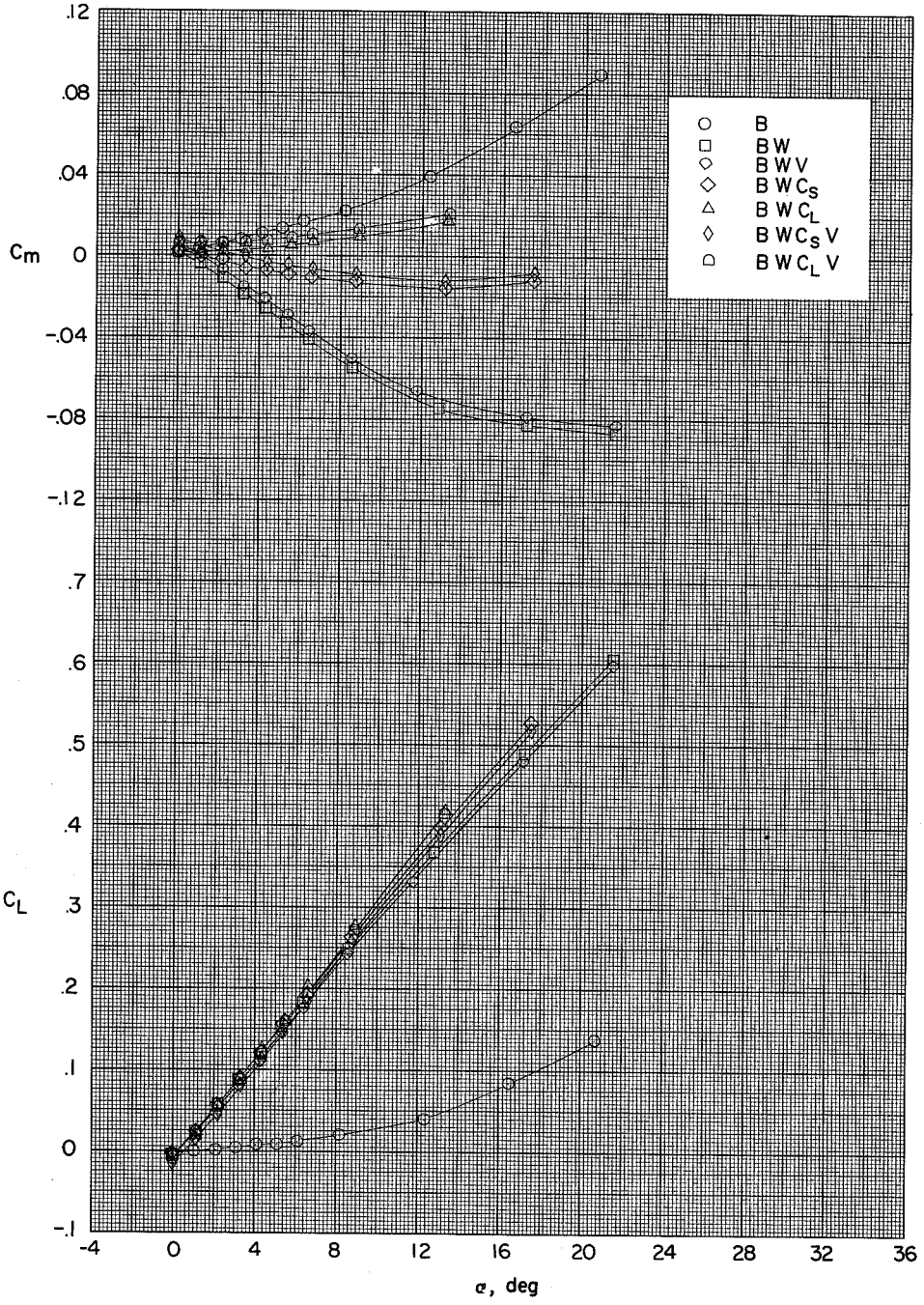


(b) Long body.

Figure 3.- Continued.

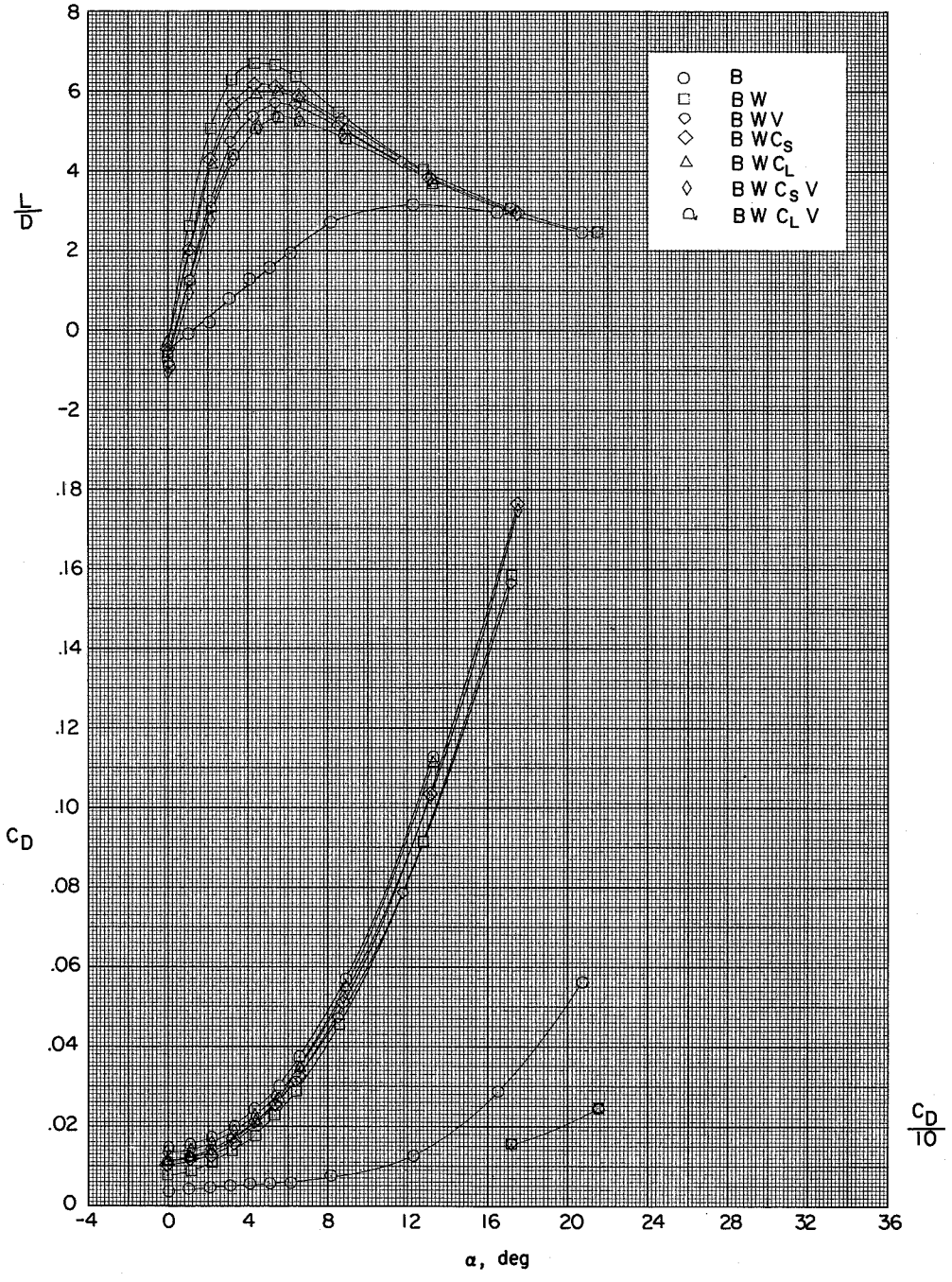


(b) Concluded.

Figure 3.- Concluded.

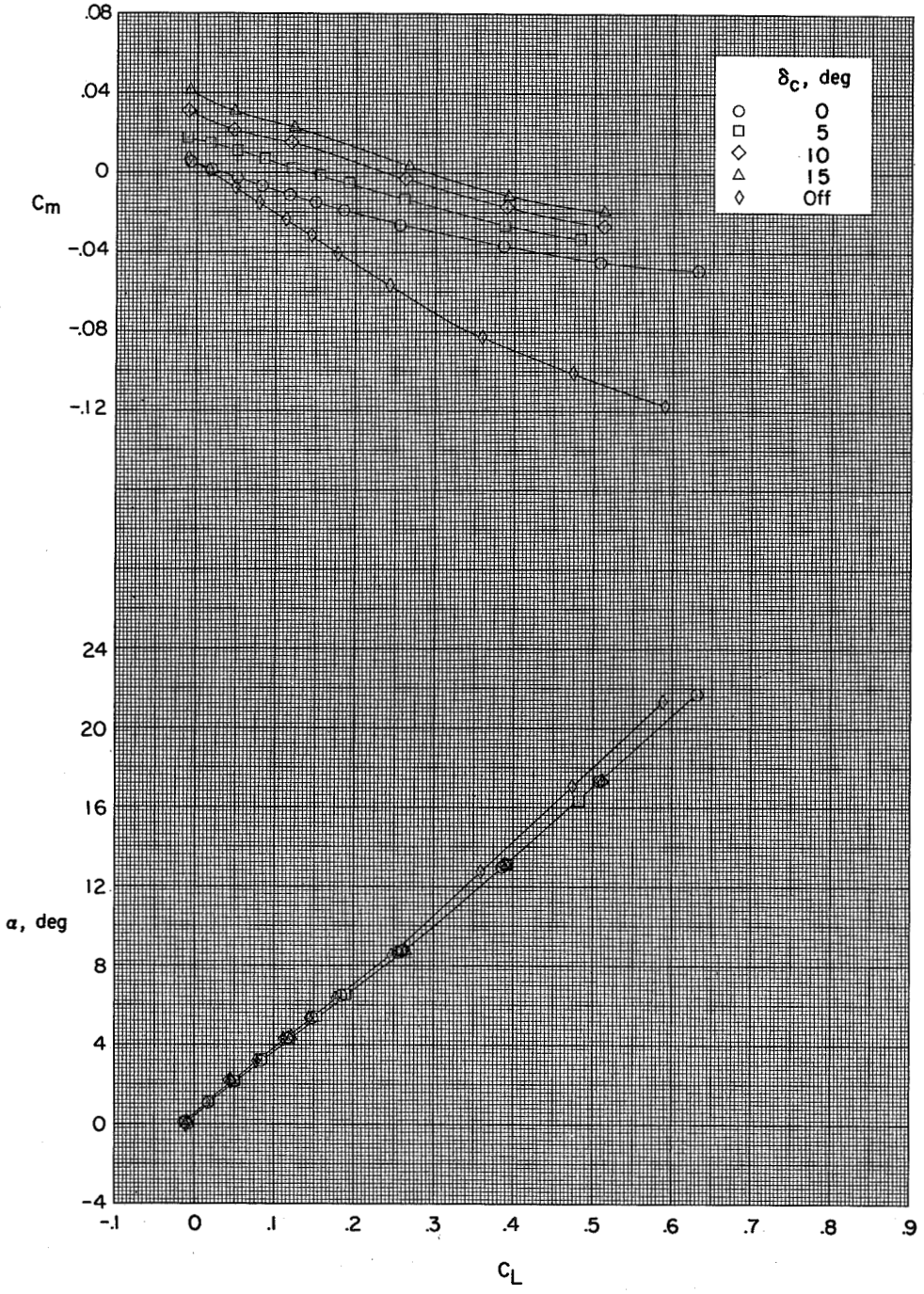


(a) Short body and small canard surface.

Figure 4.- Effect of canard-control deflection on aerodynamic characteristics in pitch for two body lengths and two canard sizes.

CONFIDENTIAL



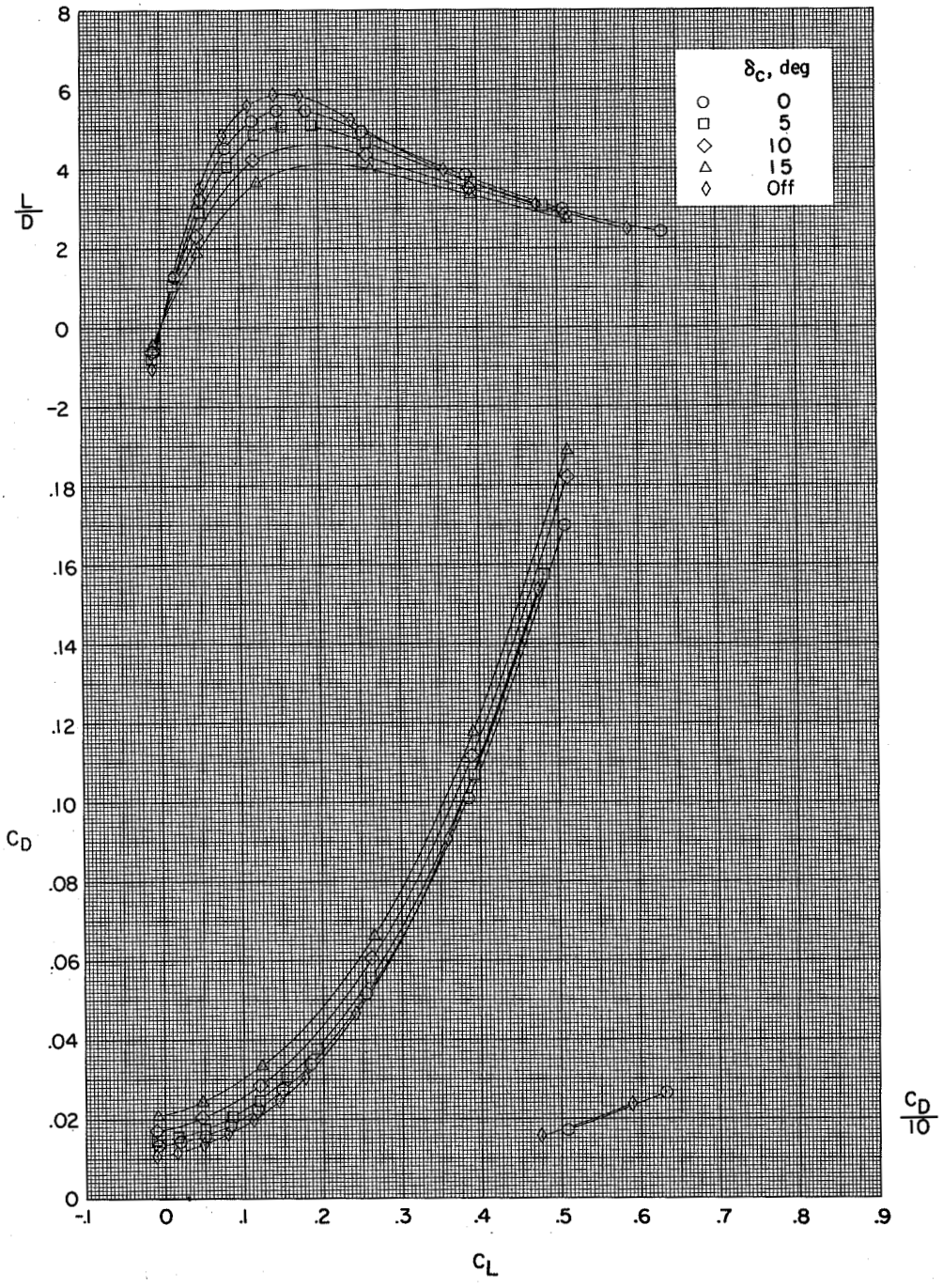


(a) Concluded.

Figure 4.- Continued.

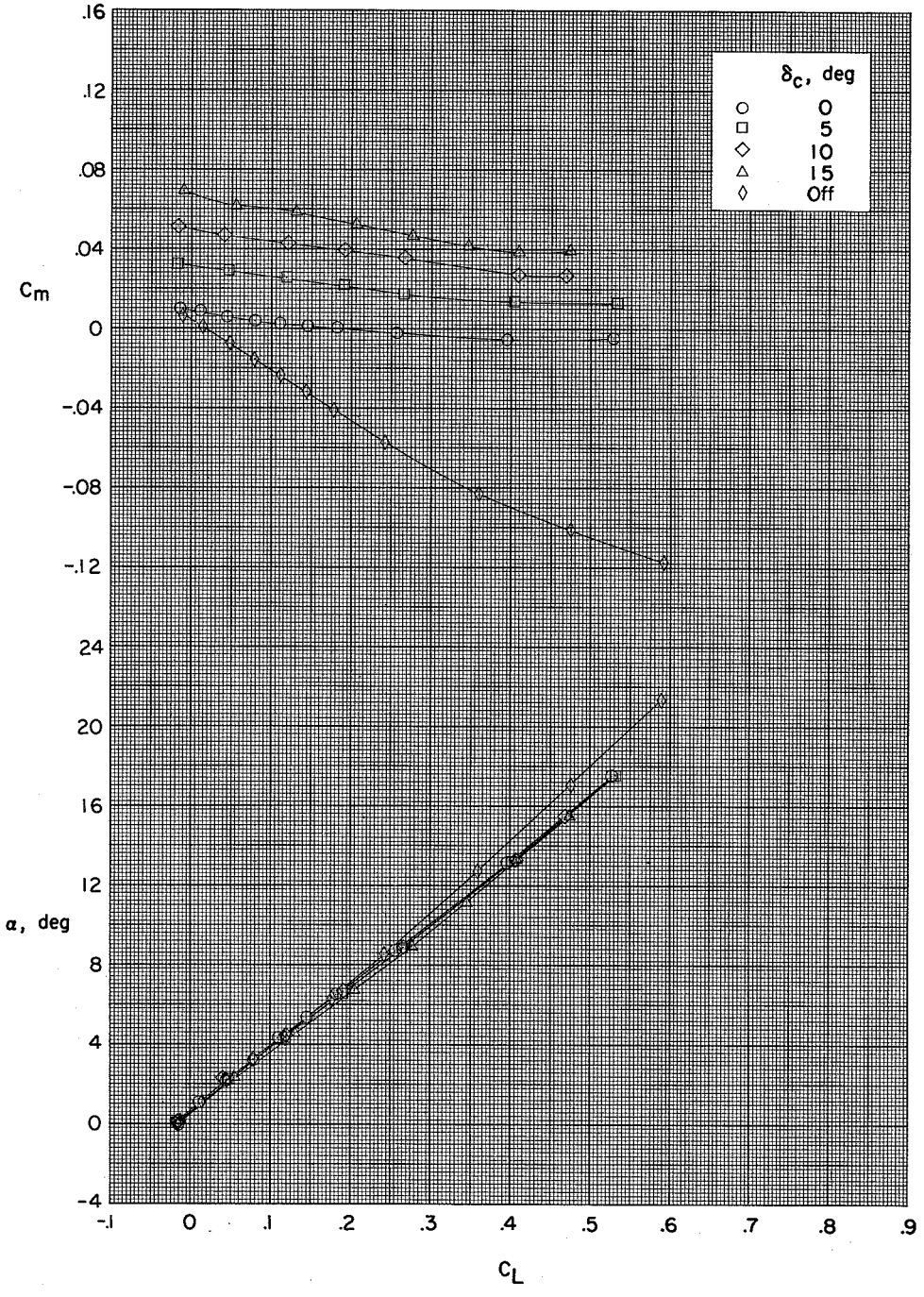


(b) Short body and large canard surface.

Figure 4.- Continued.

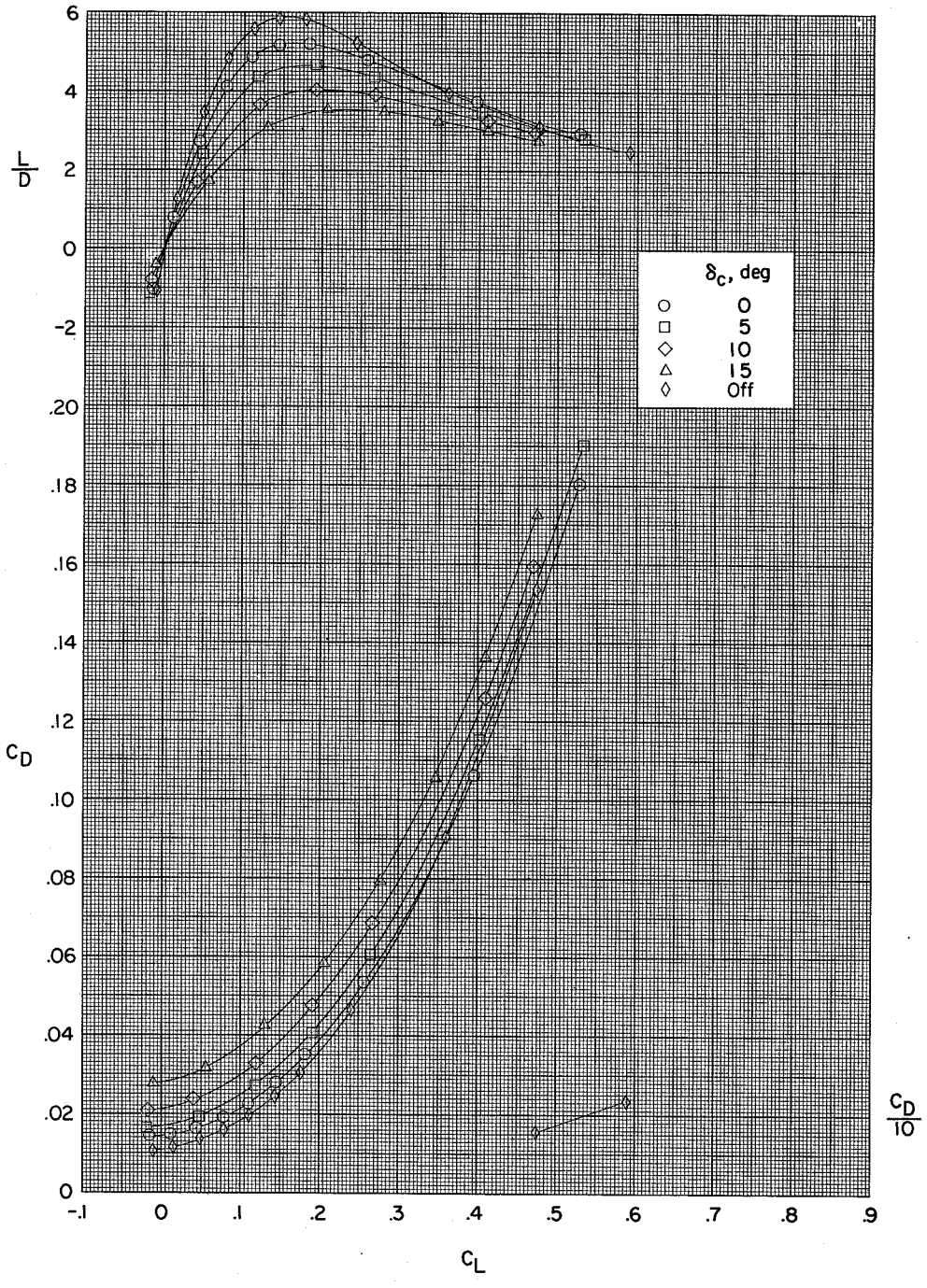


(b) Concluded.

Figure 4.- Continued.

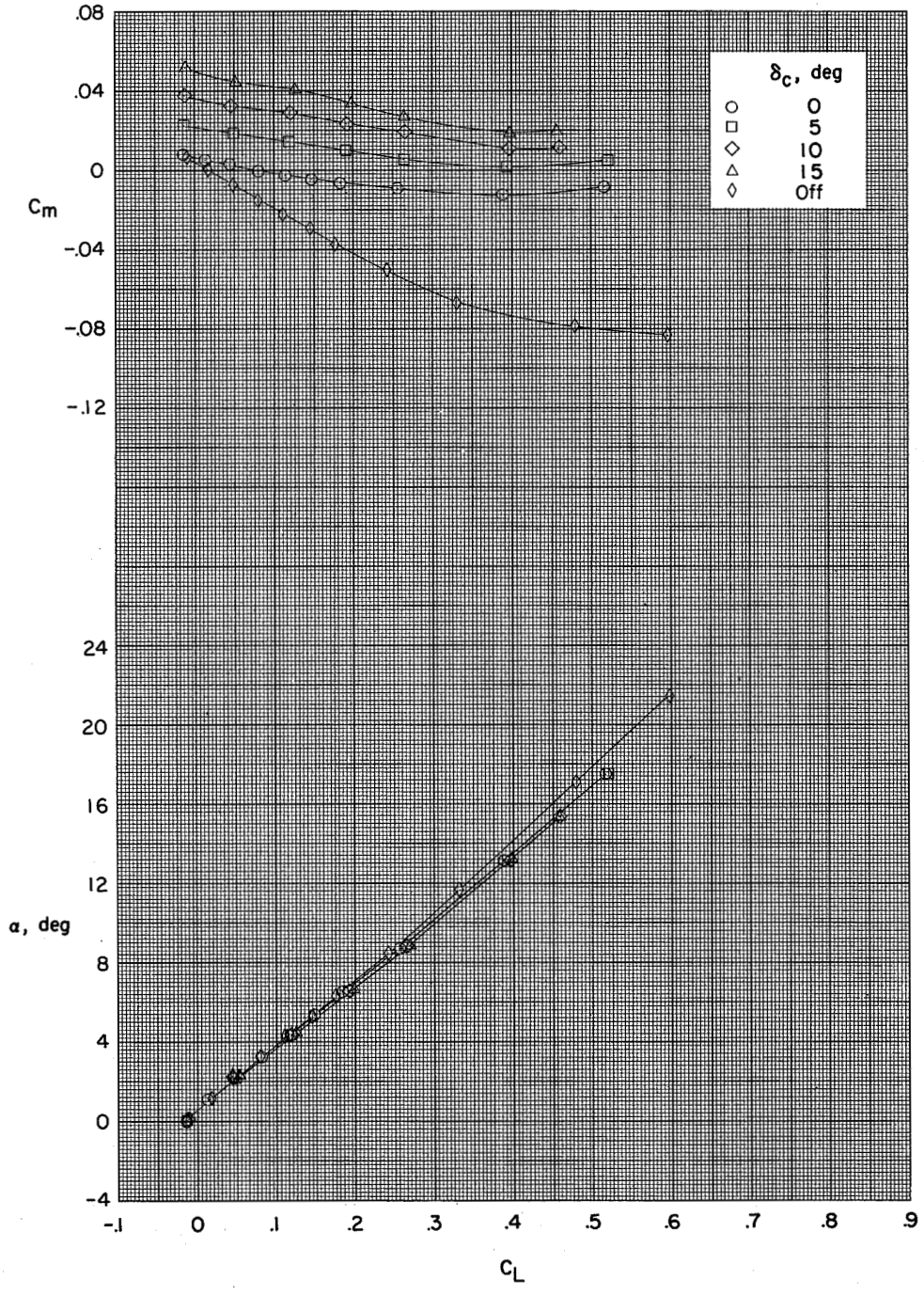


(c) Long body and small canard surface.

Figure 4.- Continued.

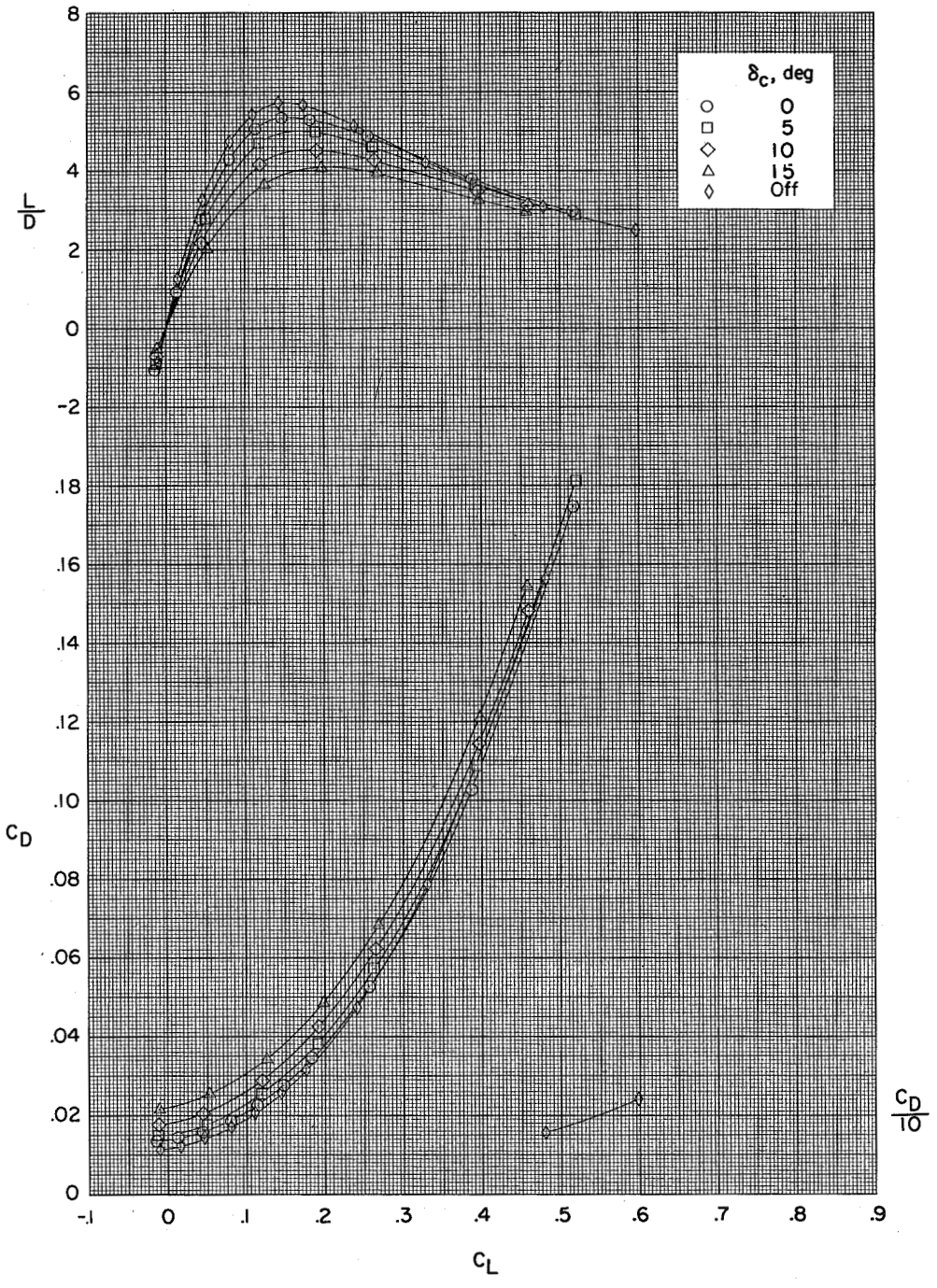


(c) Concluded.

Figure 4.- Continued.

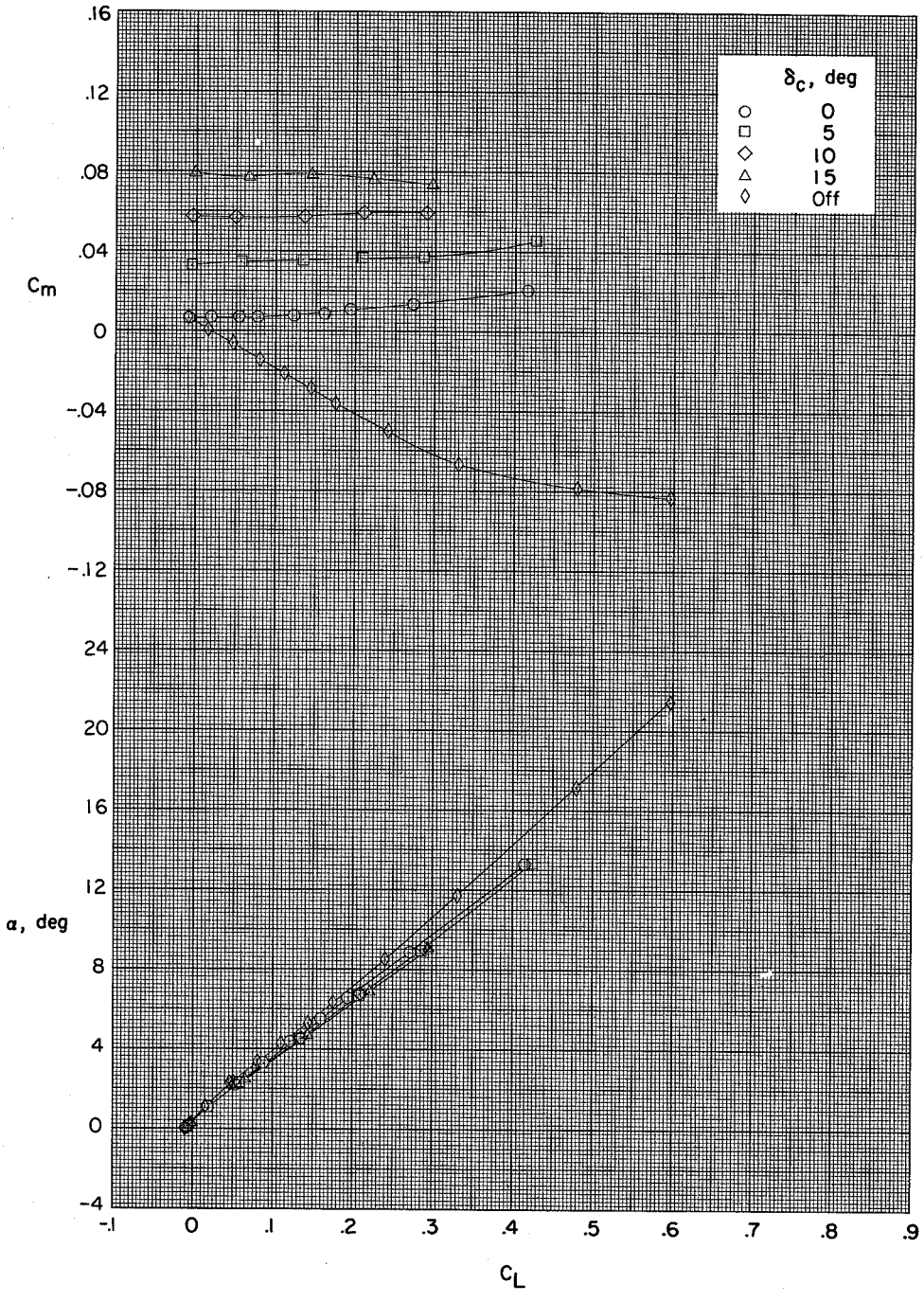


(d) Long body and large canard surface.

Figure 4.- Continued.

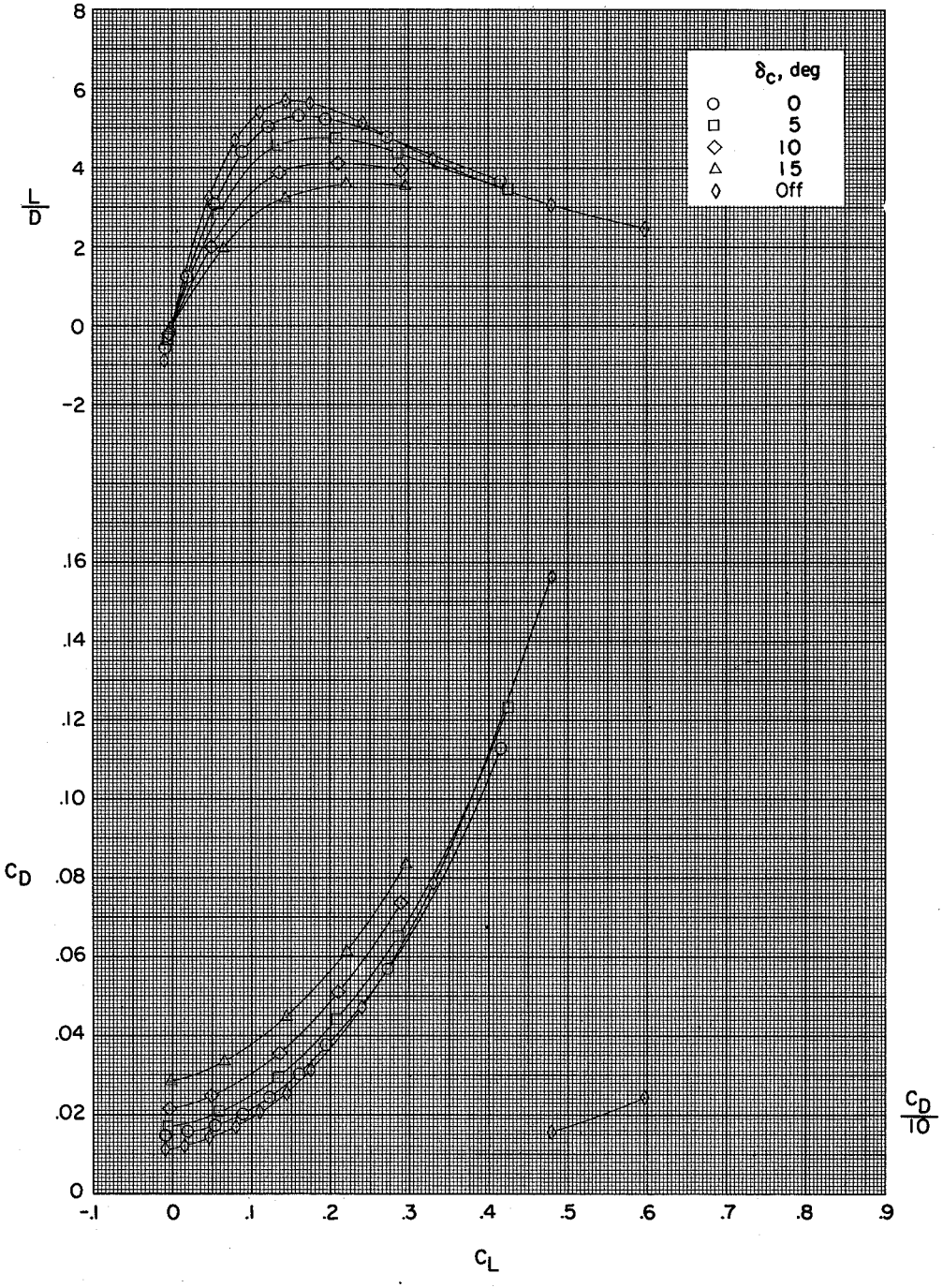


(d) Concluded.

Figure 4.- Concluded.

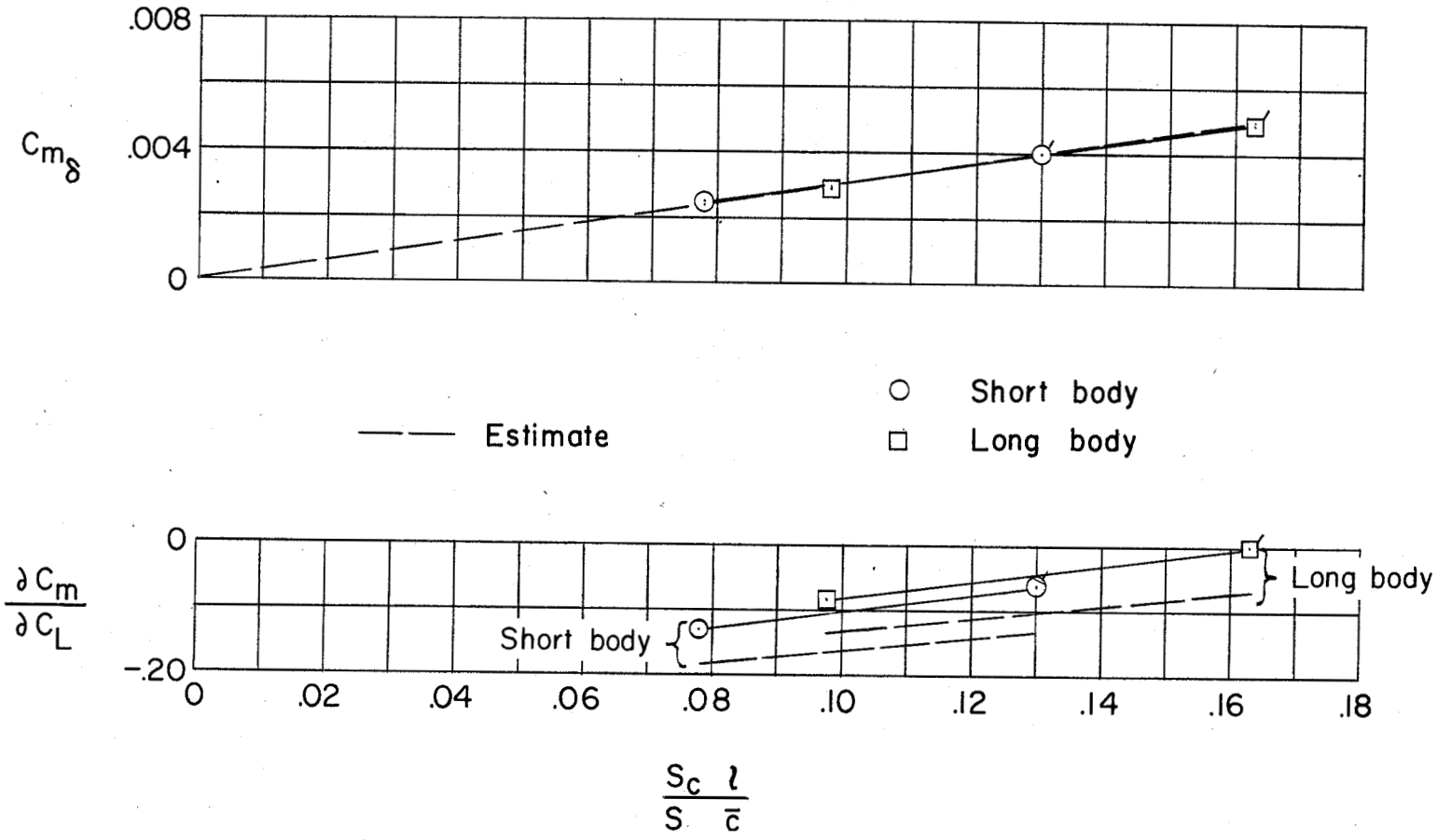


Figure 5.- Variation of canard pitching effectiveness and static longitudinal stability with canard volume coefficient. Flagged symbols are for large canard surface.

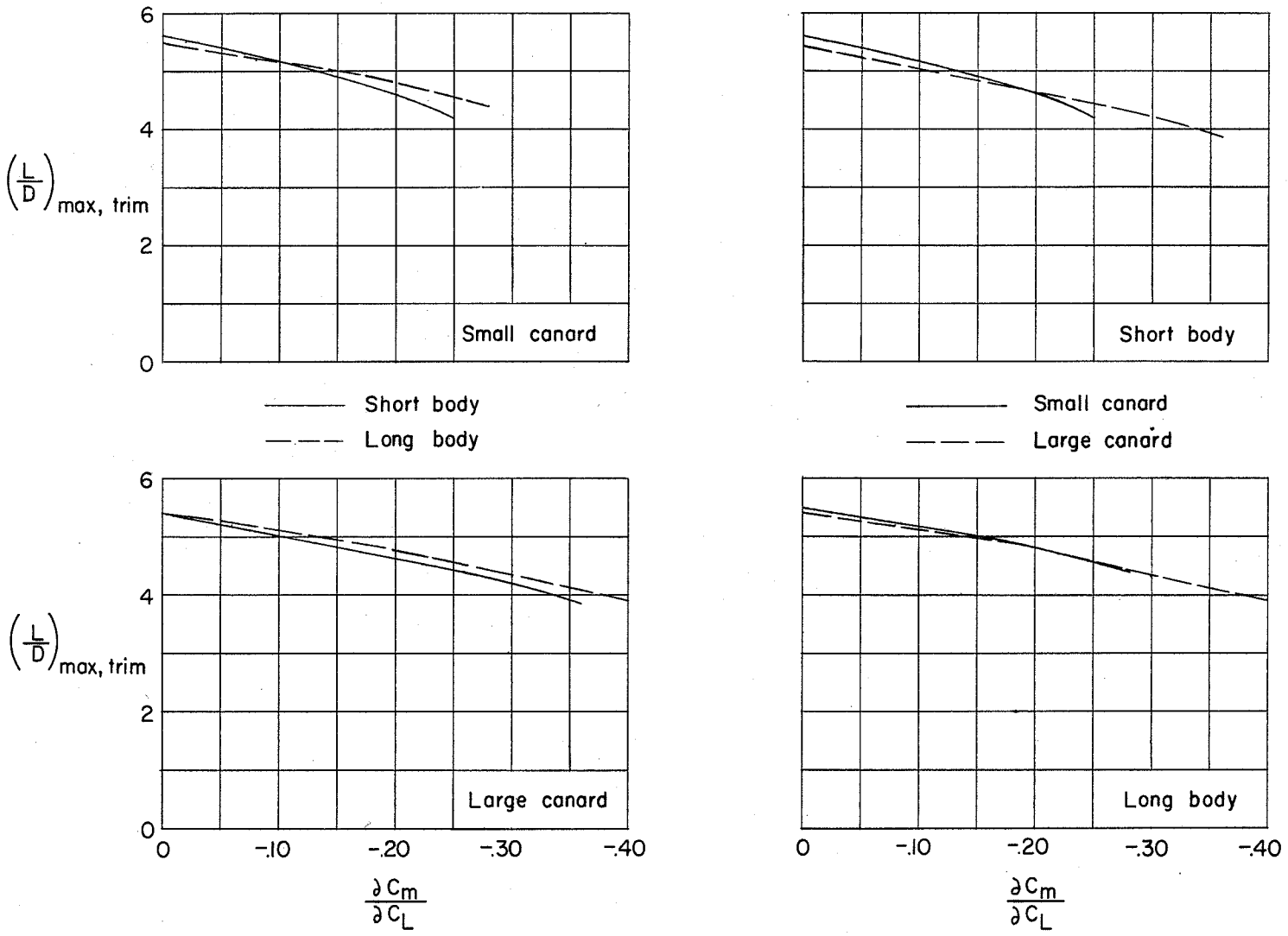


Figure 6.- Variation of maximum trim L/D with static longitudinal stability.

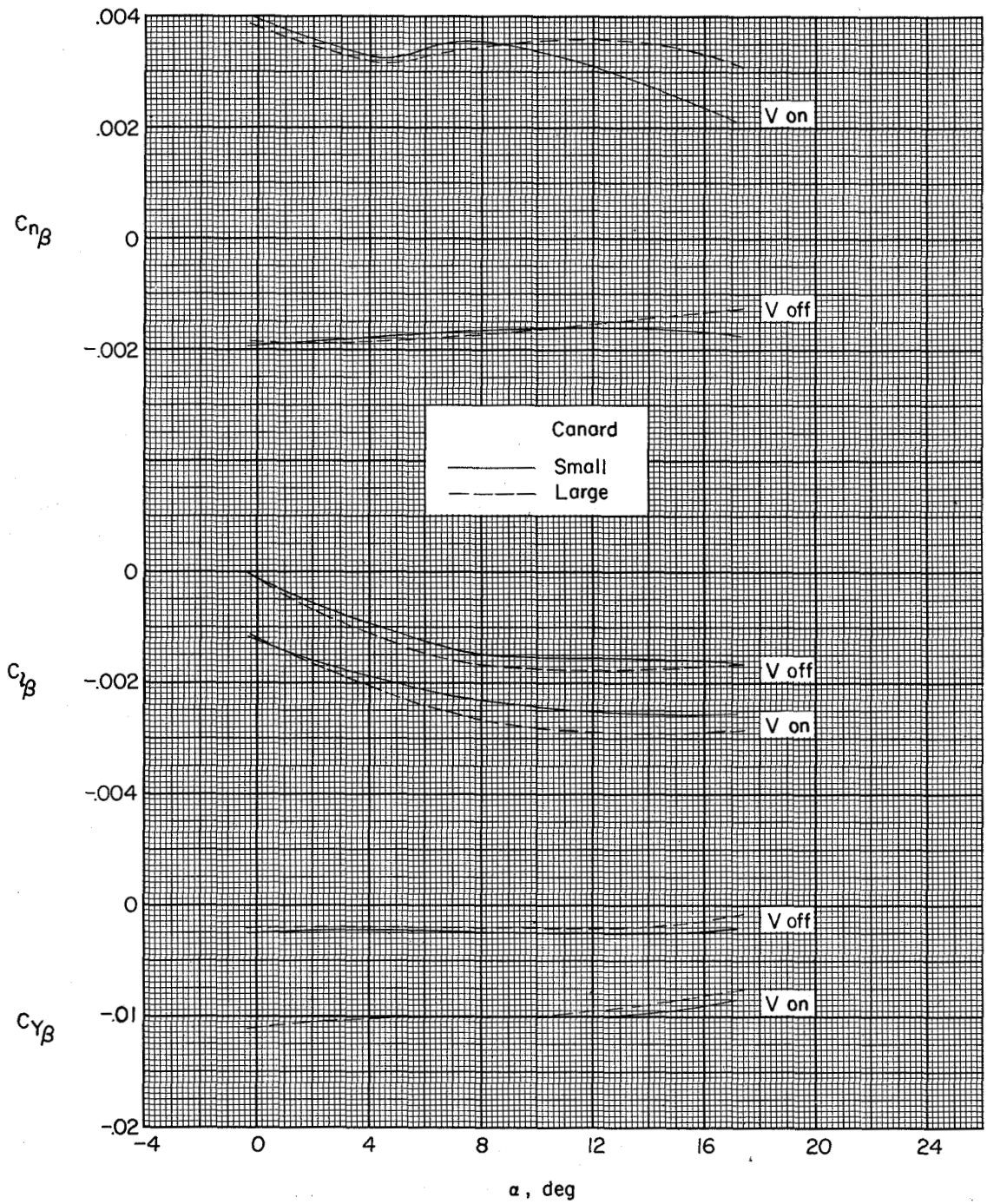


(a) Short body.

Figure 7.- Effect of canard-surface size on sideslip derivatives.

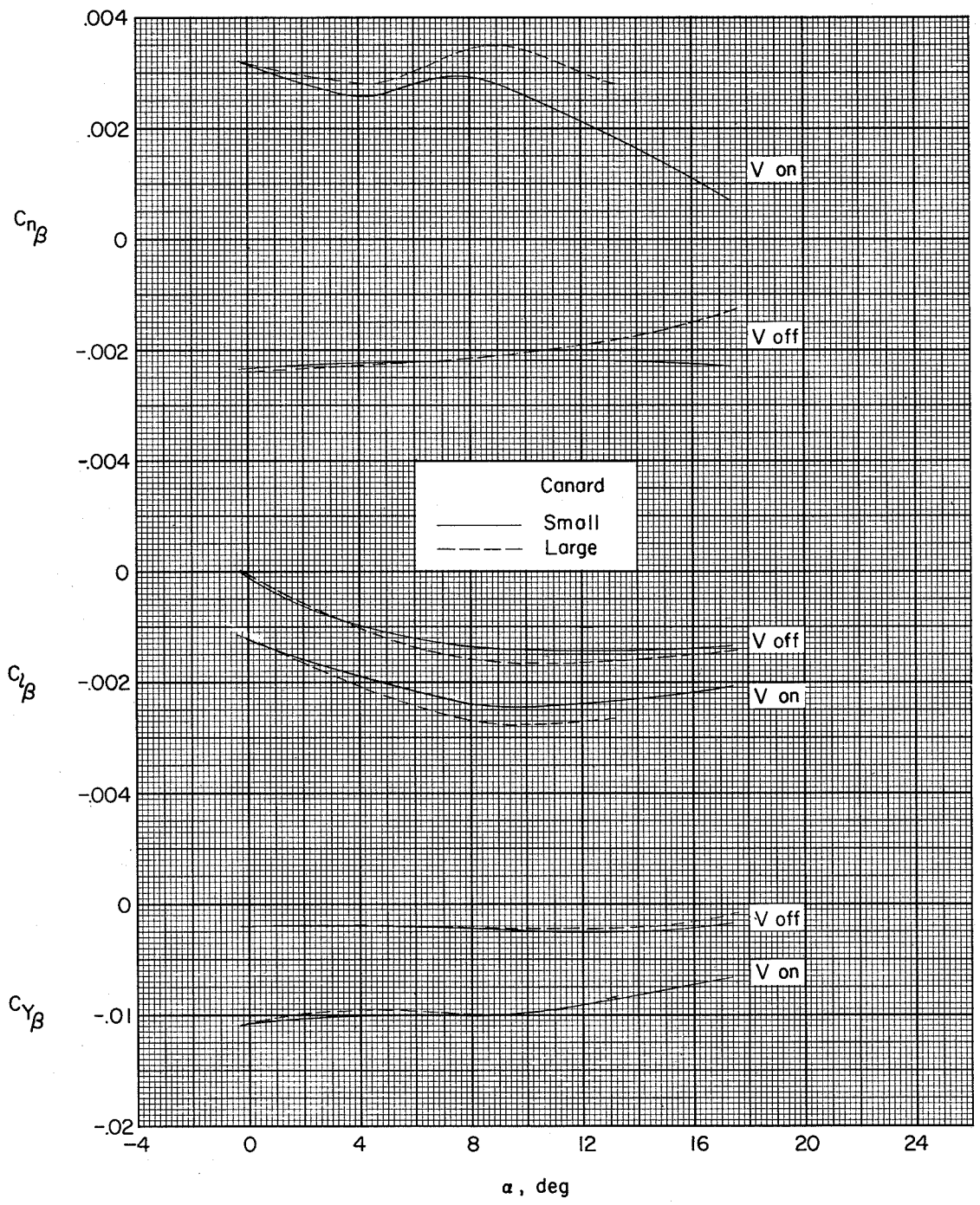


(b) Long body.

Figure 7.- Concluded.

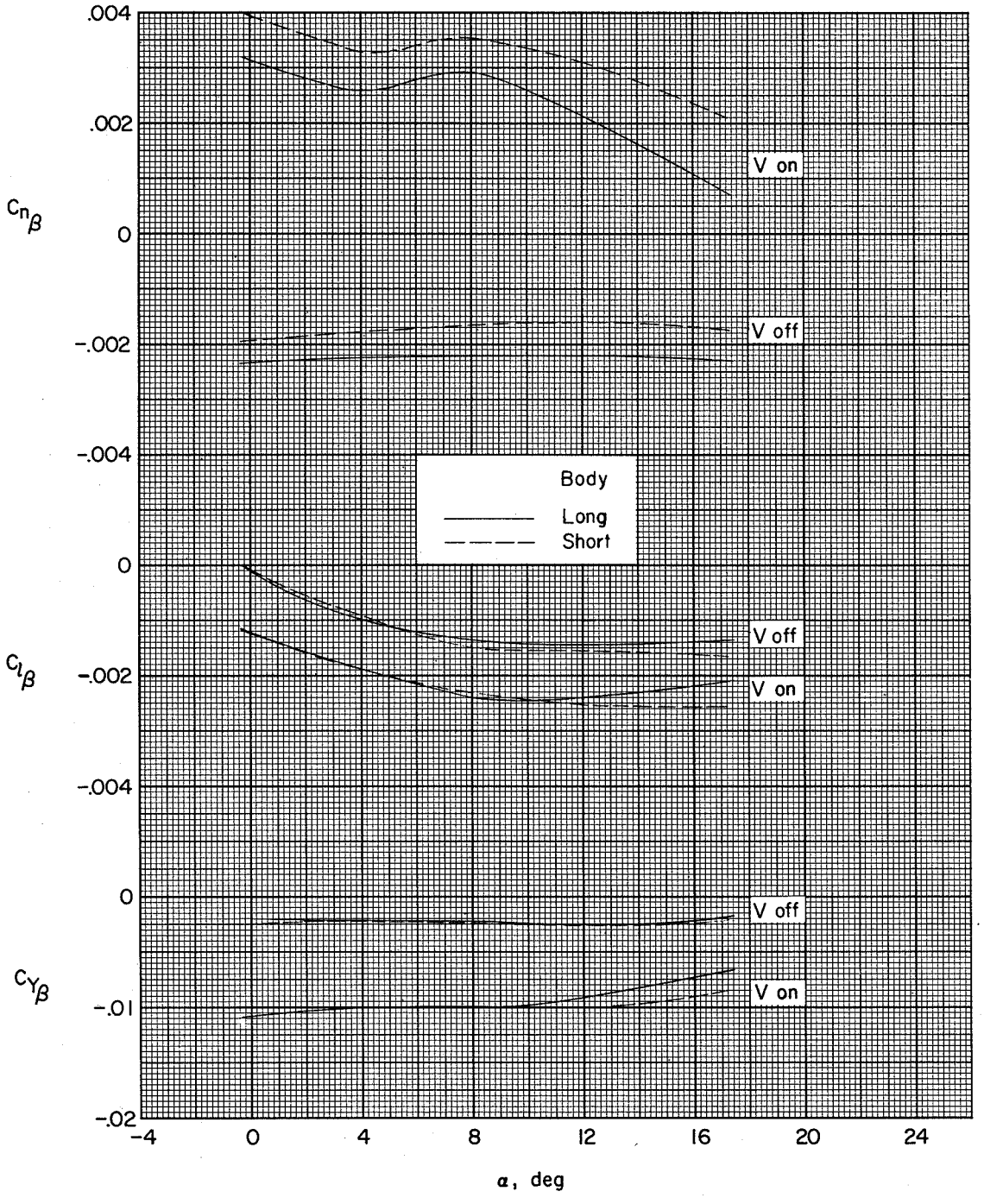


(a) Small canard surface.

Figure 8.- Effect of body length on sideslip derivatives.

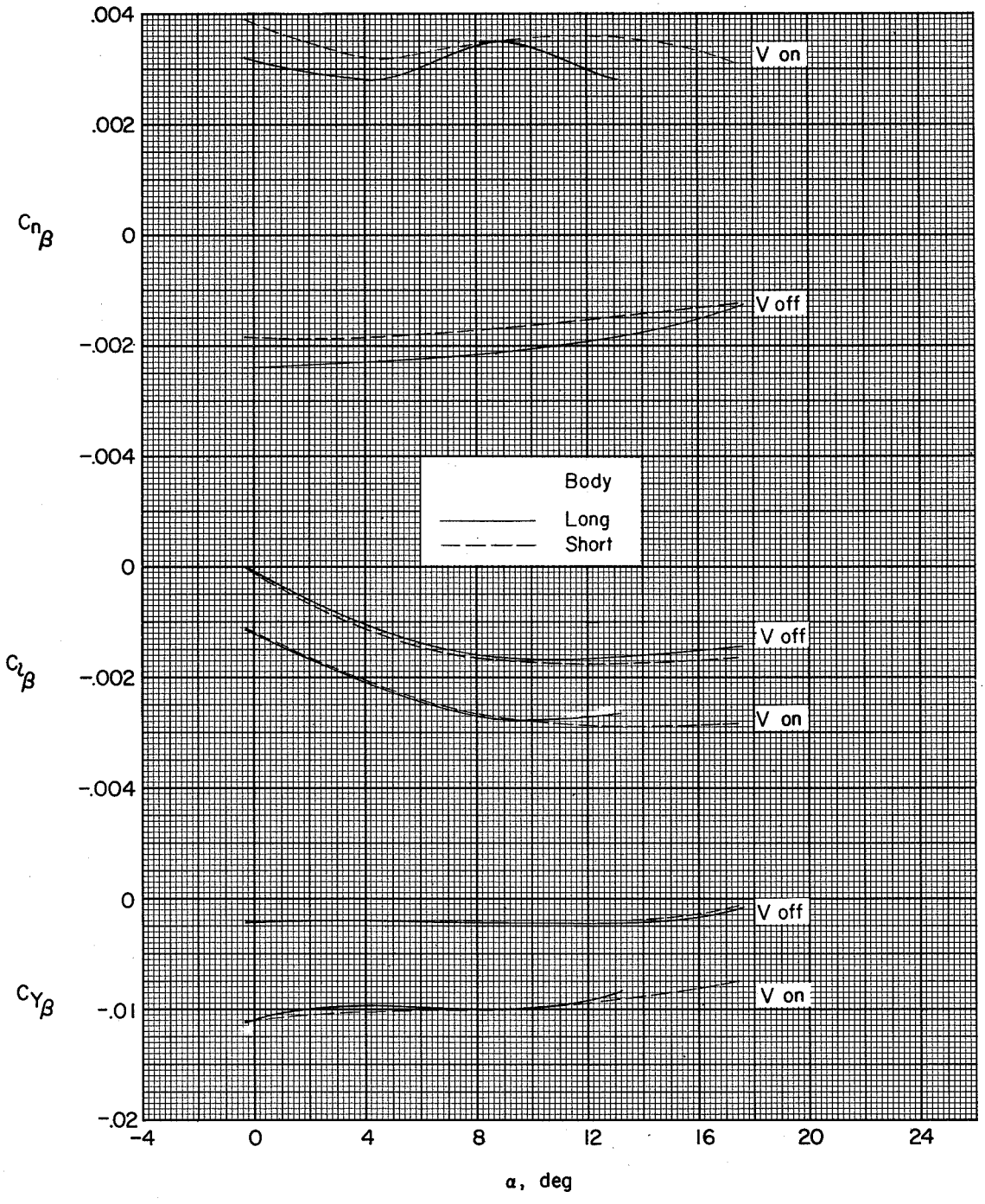


(b) Large canard surface.

Figure 8.- Concluded.